Far East Journal of Applied Mathematics
Volume 76, Number 1, 2013, Pages 39-61
Published Online: May 2013
Available online at http://pphmj.com/journals/fjam.htm
Published by Pushpa Publishing House, Allahabad, INDIA

MEASUREMENT OF DISCHARGE COEFFICIENT OF FLOW IN SHARP-EDGED CYLINDRICAL ORIFICES

Nord-Eddine Sad Chemloul

Department of Mechanical Engineering
University Ibn Khaldoun
Tiaret 14000, Algeria

Abstract

In this experimental study, discharge coefficients for flow through small sharp-edged cylindrical orifices of diameters between 1 and 0.0984 in and aspect ratios between 1 and 40 are measured. For the determination of the flow characteristics, three regions are considered; separated, attached and cavitated flow regime. The results show that while the discharge coefficient scales with the Reynolds number and aspect ratio in the attached flow regime, the diameter influences the discharge coefficient in the separated flow regime. The onset of cavitation in the orifice is also seen to be dependent on the diameter and aspect ratio. The hysteresis in the flow and the violent disintegration of the jet observed for an aspect ratio of about 5 are discussed.

1. Introduction

Sharp-edged cylindrical orifices are used for metering flows and for injecting liquid fuels into combustion chambers at high velocities. Sharp-

2010 Mathematics Subject Classification: 76-XX.

Keywords and phrases: sharp-edged orifices, discharge coefficient, attached flow, cavitated flow.

Communicated by K. K. Azad

Received January 5, 2013

edged orifices are preferred over shaped orifices for the different applications. Hobbs and Humphreys [1] and Ohrn et al. [2] have addressed the orifice geometrical effects upon discharge coefficients. Rounding of the inlet edges of the orifice was seen to increase the discharge coefficient. Small changes in the entrance curvature not only caused drastic variations of the discharge coefficient but also significantly altered the structure of the liquid jet formed (Wu et al. [3]). Further, the fabrication of the shaped orifices is difficult. For the experimental study of the discharge coefficient, a very interesting investigation was carried out by Hollingshead [4]. In the present paper the characteristics of flow through small sharp-edged cylindrical orifices are investigated.

Studies on the disintegration of liquid jets by Wu et al. [3] show that the disturbances generated in the orifice under certain conditions of flow drastically influence the break up of the liquid jets. The growth of waves on the surface of liquid jet arising from the instability, due to the interaction of aerodynamic shear and liquid flow, is not very effective in disintegrating the jet compared to the disturbances generated in the orifice (Mansour and Chigier [5] and Tamaki et al. [6]). The disturbances generated in the orifice are primarily from the dynamic effects associated with cavitation. The dynamic effects are accompanied by rapid variations in the discharge coefficient of the orifice.

Detailed measurements of discharge coefficients have been carried out by several investigators (Kiljanski [7], Pearce and Lichtarowicz [8], Spikes and Pennington [9], Hasegawa et al. [10]). The flow in the orifice is categorised as separated flow, reattached flow and cavitated flow and is illustrated in Figure 1. The separated and cavitated flows give small values of discharge coefficient in view of the contracted area of flow. For the study of cavitation flows through the orifices, we can also refer to Tamaki [11], Hiroyasu [12], Takahashi et al. [13] and Zhang and Chai [14], Chandan and Yoav [15], Ahn et al. [16], Dabiri et al. [17]. For recent works, see references [18] to [22]. The Reynolds number, defined with the characteristic dimension as the orifice diameter, typically varies in the range 10^4 to 10^7 in most fuel

injection orifices. However, turbulent flow is not likely to develop considering the short distance of flow in the orifice.

The discharge coefficients at the higher values of Reynolds number (exceeding about 2×10^5) have been shown to be insensitive to variations of Reynolds number (Pearce and Lichtarowicz [8]) for the reattached flow regime shown in Figure 1. Pearce and Lichtarowicz [8] found the values of the discharge coefficient C_d at these higher ranges of Reynolds number as a function of the aspect ratio L/d to be:

$$C_d = 0.827 - 0.0085\frac{L}{d}, \tag{1}$$

where L and d are respectively the length and the diameter of the orifice.

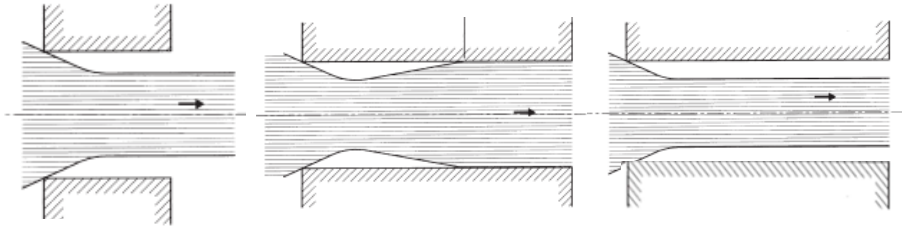

(a) (b) (c)

Figure 1. Form of the flow in the orifice: (a) separated flow, (b) separated flow followed by attachment, (c) cavitated flow.

The discharge coefficients have also been determined (Pearce and Lichtarowicz [8]) for separated flows in terms of cavitation number $(1/\sigma_c)$ and a contraction coefficient C_d for sharp-edged. It is shown that:

$$C_d = C_c\left(1 + \frac{1}{\sigma_c}\right)^{1/2}, \tag{2}$$

where C_c is the coefficient of contraction, which for sharp-edged entry orifice is equal to 0.62. The cavitation number $(1/\sigma_c)$ is defined in terms of the dynamic pressure producing cavitation to the static pressure opposing it

and is given by:

$$\frac{1}{\sigma_c} = \frac{P_i - P_a}{P_a - P_v} \tag{3}$$

with P_i the inlet pressure to the orifice, P_a the exit pressure which is equal to the ambient value, and P_v the vapour pressure of the liquid.

Though the discharge characteristics of sharp-edged orifices are reasonably well catalogued for both the cavitated and the reattached flows, it has not been possible to explain the experimental observations of the dependence of discharge coefficients on orifice diameters and the spontaneous disintegration of liquid jets observed with orifices with aspect ratios near 5. The experiments of Arai reported by Karasawa et al. [23] and Ramamurthi and Nandakumar [24] show the liquid jets, formed in sharp-edged orifices with aspect ratio around 5, to disintegrate spontaneously at certain critical values of Reynolds number. The recent flow visualisation studies of cavitating and noncavitating flows in orifices by Tamaki et al. [6] bring out the importance of cavitation-induced disturbances for an aspect ratio of 4. However, their flow visualisation studies are restricted to orifice diameters of 1 mm and 1.5 mm and aspect ratios of 2.5, 4 and 20. The link, if any, between discharge coefficient variations and disintegration cannot be evaluated from their experiments.

Experiments are therefore conducted in the present investigation with sharp-edged orifices of diameters varying about an order of magnitude at different aspect ratios. Smaller values of diameters between 1 and 2.5 mm are chosen. Injection orifices, used for diesel engines and liquid propellant rocket chambers generally conform to these small ranges of diameters. The small diameter orifices are also used for metering flows (Spikes and Pennington [9], Hasegawa et al. [10], Karasawa et al. [23], Ramamurthi and Nandakumar [24], Washio et al. [25]). The variations in discharge coefficients and the disintegration pattern of the jet formed are studied. The influence of diameter and aspect ratio variations on discharge coefficient and the disintegration pattern are determined. The motivation for the study is to obtain a better understanding of the flow pattern in the attached and separated flow regimes

in sharp-edged orifices and help in recommending the choice of aspect ratio, size of the orifice and Reynolds number of operation for different applications.

2. Experiments

Sharp-edged cylindrical orifices of diameters 1.0, 1.5, 2.0 and 2.5 mm are chosen for the experiments. The aspect ratios of the orifices are varied between 1 and 40. The orifices are formed using high-speed drill with drilling being carried out from orifice exit face to prevent formation of burs at the orifice entry. Ohrn et al. [26] have shown that variations in the nature of sharp-edged entry can give rise to considerable variations in the discharge coefficient.

The experiments are done with demineralised water. The experimental set-up comprises of a tank with water, nitrogen gas source for pressurising the water and a feed-line fitted with flow control valves for supplying water at pressures between 0.05 and 1.5 MPa to the orifice. The contraction ratio between the supply manifold and the orifice is kept less than 0.4. The manifold diameter is 10 mm. This is done based on experimental findings (Bergwerk [27]) that the discharge characteristics of the orifices are not influenced by the size of the supply manifold when the contraction ratio is less than 0.5.

The orifice discharges into the ambient atmosphere. The shape of the jet is determined by direct photography using a high-speed strobe flash. The discharge coefficient is calculated using the relation:

$$Q_v = C_d S \sqrt{\frac{2\Delta p}{\rho}} \tag{4}$$

with Δp the pressure drop across the orifice, ρ the density of water which is $1000\text{kg}/\text{m}^3$, S the orifice area, Q_v the volumetric flow rate and C_d the discharge coefficient. In this equation the flow velocities in the supply are neglected. However, for small contraction ratios of the experiment, the dynamic pressure head is negligible compared to the pressure drop in the orifice and the use of equation (4) is justified.

The Reynolds number R_e of the orifice flow is defined with the diameter d of the orifice by:

$$R_e = \frac{\rho U d}{\mu}, \tag{5}$$

where U is the flow mean velocity, and μ is the viscosity of water.

The pressure upstream of the orifice is measured using a digital pressure gauge. The uncertainty in the measurement of pressure is ± 0.002 MPa. The discharge rate through the orifice Q_v is measured by collection over a period of time and the uncertainty in the measurement is 1 cc/s. The overall uncertainty in the measurement of discharge coefficient in the present experimental set-up is therefore estimated to be less than ± 0.8% when Δp is greater than 0.2 MPa. However, in the region where injection pressure drops below about 0.05 MPa, a relatively large proportion of errors in pressure measurement would lead to enhanced error in the discharge coefficients.

3. Results and Discussions

3.1. Aspect ratio effect on discharge coefficient

Figure 2 gives the observed variations of discharge coefficient with Reynolds number for orifices of diameters 1 and 2.5 mm, respectively. The results of two diameters are chosen for illustrating the trends of variation of discharge coefficients for the different aspect ratios of the orifices since they represent the smallest and largest diameter of orifice used and bring out clearly the role of changes in diameters on the discharge coefficient. To analyse the results of Figure 2, three domains of the aspect ratio were considered:

3.1.1. Case a $(L/d = 1)$

The flow through the orifices would get separated from the wall as indicated in Figure 1 when the aspect ratio of the orifice is unity. Small values of discharge coefficient obtained at aspect ratio of unity for 1 and 2.5 mm orifices (Figure 2) do confirm that the flow is separated. The jet issuing

from the orifice is also unruffled suggesting free separated flow and this will be dealt with subsequently.

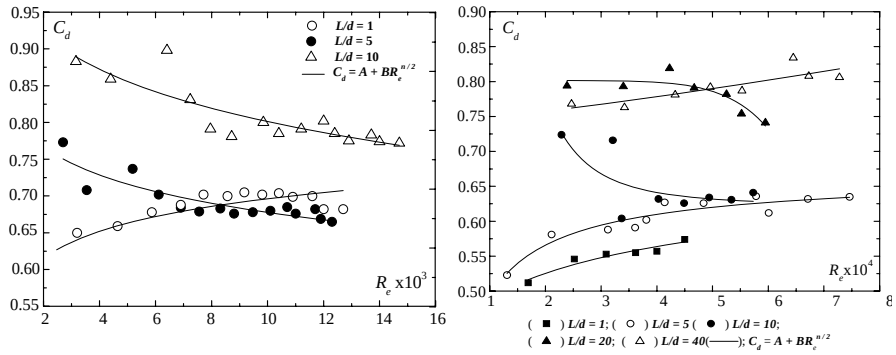

(a) (b)

Figure 2. Variation of discharge coefficient diameter orifice at different aspect ratios: (a) $d = 1\,\text{mm}$; (b) $d = 2.5\,\text{mm}$.

The discharge coefficient for the 2.5 mm orifice is seen to be reasonably constant over the range of Reynolds number investigated $(2 \times 10^4 < R_e < 4.5 \times 10^4)$. Similar result was obtained by Chun Lang [28]. In the case of the 1 mm orifice the discharge coefficient decreases with increasing Reynolds number when the Reynolds number is between 3×10^3 and 6×10^3 and remains constant thereafter.

Variations in discharge coefficient are not to be anticipated when the Reynolds number changes for separated flows. The pressure drop across the orifice is mainly due to the pressure loss at the orifice entry and is proportional to the dynamic head $\rho U^2/2$. The observation of near constant discharge coefficient at $R_e > 6 \times 10^3$ for the 1 mm orifice, and for $2 \times 10^4 < R_e < 4.5 \times 10^4$, for the 2.5 mm orifice is therefore to be anticipated. The increase of C_d when R_e decreases to the values below 6×10^3 for the 1 mm orifice suggests a pressure drop less than that associated with the entry pressure loss.

The contribution of pressure by surface tension pumping for the small orifice is $2\sigma/r$, with r is the radius of the orifice. This driving pressure for a surface tension coefficient of 0.072 N/m for water is about 0.001 MPa for the 1 mm orifice. This is one order of magnitude less than the minimum inertial pressure drop of 0.02 MPa corresponding to the lower regimes of Reynolds number in Figure 2. However, this is sufficient to contribute to increase the discharge coefficient by about 14%. The effect is particularly predominant at the smaller values of inertial pressure drops and is responsible for the observed increase of discharge coefficients at small values of Reynolds number in the case of the small orifice diameters. When the orifice diameters are larger, the surface tension induced pressures are negligible leading to near-constant values of the discharge coefficients.

3.1.2. Case b $(L/d = 5)$

When the aspect ratio of the orifice is 5, the value of the discharge coefficient for both 1 and 2.5 mm orifices initially increases with increase of Reynolds number, reaches a maximum and then abruptly drops to values corresponding to separated flows. When the Reynolds number is increased beyond values at which separation takes place the discharge coefficient remains reasonably constant. This trend is shown in Figure 2. The initial increase of the discharge coefficient with increase of Reynolds number is understandable based on the pressure drop for the reattached flow through the orifice. The frictional pressure drop in the attached region of flow is given by:

$$\Delta P_f = \rho \frac{4 f L U^2}{2d}, \tag{6}$$

where f is the friction coefficient. The total pressure drop in the orifice is the sum of the pressure loss at orifice entry and the frictional pressure drop within the orifice, which can be stated as:

$$\Delta P = \rho \frac{4 f L U^2}{2d} + k \frac{\rho U^2}{2}. \tag{7}$$

Here k is the coefficient for entry pressure loss. The variation of the skin

friction coefficient *f* with Reynolds number can be approximated as:

$$f = \frac{C}{R_e^n}, \tag{8}$$

where *C* and *n* are constants. Substituting the above value of *f* in equation (7), we get the following expression for the discharge coefficient:

$$C_d = A + BR_e^{n/2}, \tag{9}$$

where *A* and *B* are constants. The value of *n* is typically 0.5 for laminar flow and about 0.2 for turbulent flow. The discharge coefficient should therefore increase with increase of Reynolds number which is observed in the experiments.

When the flow gets separated due to the onset of cavitation, the discharge coefficient falls to near-constant values of about 0.68 for the 2.5 mm orifice and 0.78 for the 1 mm orifice (Figure 2b). The higher value of C_d obtained for the smaller orifices (when flow gets separated) is due to the effect of surface tension which has been justified earlier.

3.1.3. Case c $(L/d > 5)$

When the aspect ratio of the 1 and 2.5 mm orifices is increased to a value of 10, it is observed (Figure 2) that the discharge coefficient does not drop as abruptly as occurred for an aspect ratio of 5. The Reynolds number at which the flow separates is also enhanced to higher values. The cavitation bubble, formed due to the low static pressure is not strong enough to generate the separated flow through the orifice as obtained with the aspect ratio of 5. As the jet velocities are further increased and stronger cavitation bubbles are formed, the reattachment point gets shifted further downstream. When the velocity is substantial and the reduction of static pressure is such that a strong cavitation bubble can grow, a separated flow occurs. Wang and Brenn [29] have shown that the flow becomes unstable and flashes to vapour when the size of the cavitation bubble exceeds a critical threshold value. They determine this by solving the Rayleigh-Plesset equation for growth of

bubbles. The growth of bubbles is impeded by the higher back-pressure for larger aspect ratio orifices and this aspect is dealt with in flow hysteresis section.

When the aspect ratios of the orifice are increased to values between 20 and 40 for the 2.5 mm diameter orifice, there is no evidence of cavitated flow and a drop in the value of the discharge coefficient (Figure 2b). The discharge coefficient progressively increases with increase of Reynolds number, as indicated by equation (9).

The experimental results obtained on the effect of the report on the discharge coefficient are in good agreement with those found by Bikai et al. [30], for nearly the same range of the aspect ratio (L/d of 1-15) and the diameter of the orifice (d of 0.8 to 3 mm).

For the effect of the Reynolds number on the discharge coefficient, similar results are obtained by Dabiri et al. [17].

3.2. Orifice diameter effect on discharge coefficient

Figures 3-4 show the influence of the variations of the diameter of the orifice on the discharge coefficients at different values of aspect ratios. For an aspect ratio of unity, for which the flow in the orifice separates, smaller values of orifice diameter give larger discharge coefficients. This trend is illustrated in Figure 3a. The phenomenon is attributed to surface tension effects and discussed earlier. The same trend is also seen in Figure 3b for an aspect ratio of 5 for the range of Reynolds number at which the flow gets separated from the orifice wall. The discharge coefficient obtained for cavitated flow is seen to be lowest for the 2.5 mm orifice and to progressively increase as the orifice diameter decreases to 2, 1.5 and 1 mm. Similar result is obtained with aspect ratio of 20.

When the aspect ratio of the orifice is increased to 5 (Figure 3b), the increasing trend of discharge coefficients observed with attached flows is seen to fall on the same common line (shown dotted) for the 0.3, 1 and 2.5 mm orifices. Similar results are obtained with aspect ratios of 20 and 50 and are shown in Figure 4.

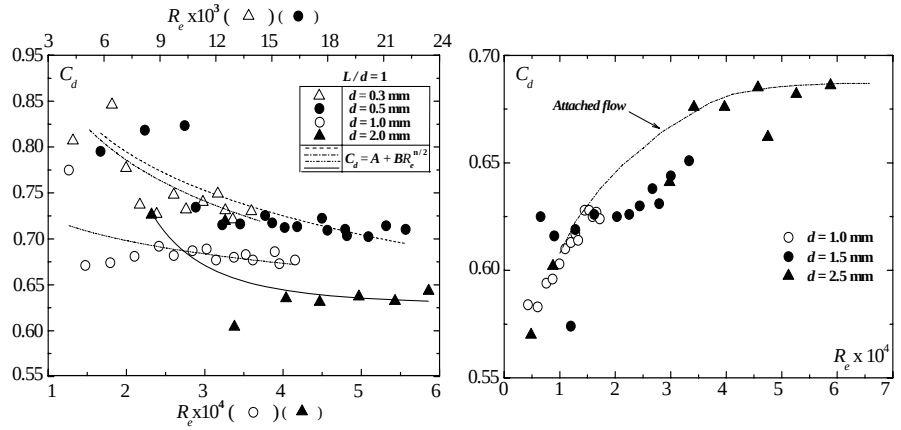

Figure 3. Variation of the discharge coefficients with the Reynolds number for different orifice diameters: (a) $L/d = 1$; (b) $L/d = 5$.

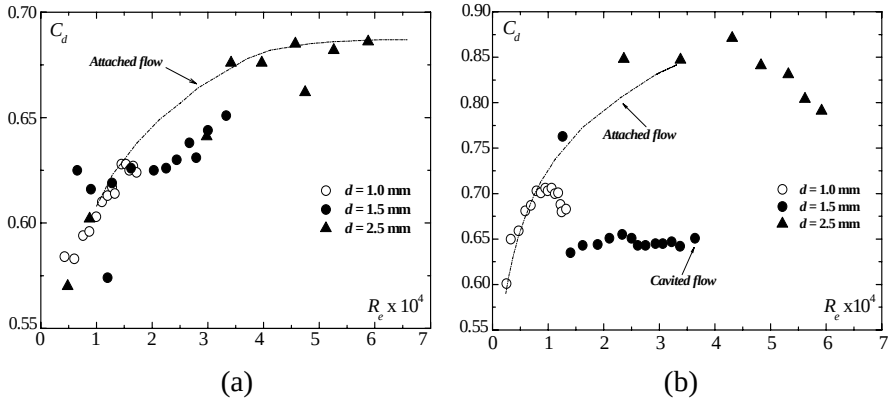

Figure 4. Variation of the discharge coefficient with the Reynolds number in attached and cavitated flow: (a) $L/d = 20$; (b) $L/d = 50$.

The values of discharge coefficient obtained in the attached flow regions before the onset of cavitation) for all values of orifice diameters and aspect ratios, are replotted in Figure 5. It is seen that the discharge coefficients for attached flows monotonically increase with increase of Reynolds number for all orifice diameters to reach about a constant asymptotic value. This maximum or upper bound value of discharge coefficient decreases as the aspect ratio of the orifice is increased.

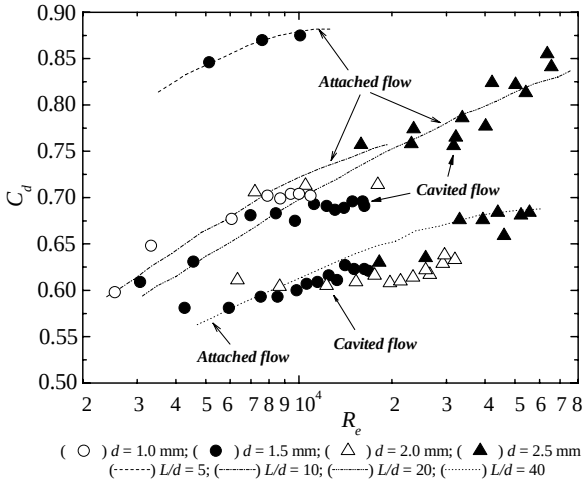

Figure 5. Variation of the discharge coefficient with the Reynolds number in attached and cavitated flow for different aspect ratios and orifice diameters.

These two observations are qualitatively similar to the findings of Pearce and Lichtarovicz [8].

The influence of orifice diameters and aspect ratios on discharge coefficient can therefore be summarised as follows. In the case of attached flow in the orifice, the discharge coefficient scales with Reynolds number for the different values of diameters of orifices.

When cavitation takes place, the discharge coefficient becomes independent of the Reynolds number. The value of the discharge coefficient for separated and cavitated flow is, however, dependent on the diameter of the orifice with the smaller orifice giving larger values of discharge coefficient when the flow is separated. This phenomenon is due to the combined influence of capillary induced pressure and the improved wetting of the walls by surface tension when orifices have small diameters.

3.3. Aspect ratio and orifice diameter effects on the onset of cavitation

Figure 6 is a plot of the critical cavitation number for the onset of cavitation at the various aspect ratios. It is seen that the critical cavitation number $(1/\sigma_{cr})$ at which cavitation starts and flow separation gets initiated,

is progressively delayed as the aspect ratio increases. The critical cavitation number is also higher for smaller diameter orifices especially when the aspect ratios are large.

We note that the trend of the experimental results of $(1/\sigma_{cr})$ is the same as that of equation (10).

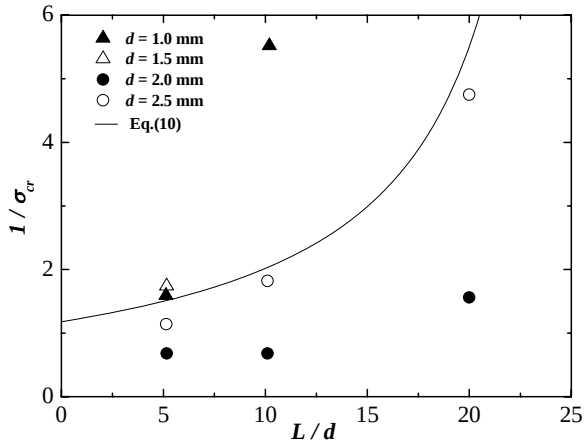

Figure 6. Variations of critical cavitation number with aspect ratio for different orifice diameters.

The reasons for the influence of orifice diameter and aspect ratio on the onset of cavitation are given below.

A schematic of the pressure drop and recovery during flow separation and the subsequent reattachment and the frictional pressure drop in the attached portion of the orifice is given in Figure 7. Orifices of two different aspect ratios are shown with the extended region of the larger aspect ratio orifices shown by dashed lines. The pressure at the exit of the orifices in both cases is the ambient pressure and is shown by points *A* and A_1 for the small and large aspect ratio orifice, respectively. The larger pressure drop in the increased reattached portion of the larger aspect ratio orifice is possible only for a higher pressure at the reattachment point. This is shown by B_1 for the orifice of larger aspect ratio and is compared with the value *B* for the smaller aspect ratio orifice in Figure 7.

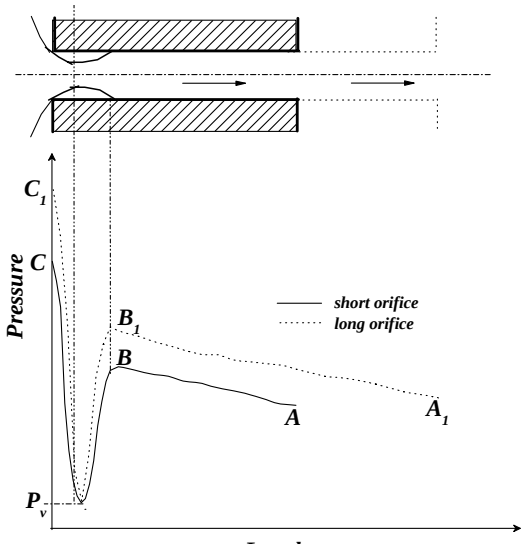

Figure 7. Pressure variation along the length of a short and long orifice.

The higher value of pressure B_1 for the larger aspect ratio orifice demands that the upstream pressure be higher to drive the same flow. The corresponding upstream pressure is denoted by C_1 and *C* for the two orifices in Figure 7 with C_1 being higher than *C*.

A higher dynamic head would be required to bring down the pressure corresponding to the higher pressure C_1 to the value of vapour pressure P_v. This implies that the cavitation number $(1/\sigma)$ (Pearce and Lichtarowicz [8]) defined by equation (3) should be larger for the larger aspect ratio orifice. This is observed in the experiments and is given in Figure 10 for aspect ratio changes between 5 and 20. It is to be noted that fully cavitated flow was not obtained for aspect ratios above 10 (Figures 6 and 7) since reattachment of flow takes place. The trend of increase of the critical cavitation number with aspect ratio is in conformity with the findings reported by Pearce and Lichtarowicz [8]) who fit the critical cavitation number as:

$$\frac{1}{\sigma_{cr}} = \frac{1.18(1 + 0.006(L/d))}{1 - 0.038(L/d)}. \qquad (10)$$

The values of the cavitation number reported in the present study are, however, higher than those predicted by the above equation. The reasons for the difference could be attributed to the smaller diameters of the orifices used. Small diameters of 1 and 1.5 mm are, in fact, seen to give higher values of critical cavitation number (Figure 6). Higher values of frictional drop associated with the smaller diameter orifices and the higher equivalent back pressure (as seen for larger aspect ratio orifices at B_1 in Figure 7) are responsible for the increase in the cavitation number. The wetting of the orifice walls by surface tension is also more pronounced in the case of smaller diameters leading to the enhancement.

3.4. Structure of the jet

The surface texture of the jet formed by the orifice has a smooth glassy appearance when the flow through the orifice is separated. The jet has a frothy milky white surface for reattached flow. The turbulent flows give the jet the milky appearance. The structure of the jet, obtained with an orifice of aspect ratio 5 at different values of Reynolds number, is shown in Figure 8. The disturbances in the jet are seen to be maximal at the Reynolds number at which the onset of cavitation occurs. The disturbances drastically reduce at the higher values of Reynolds number since the flow gets separated.

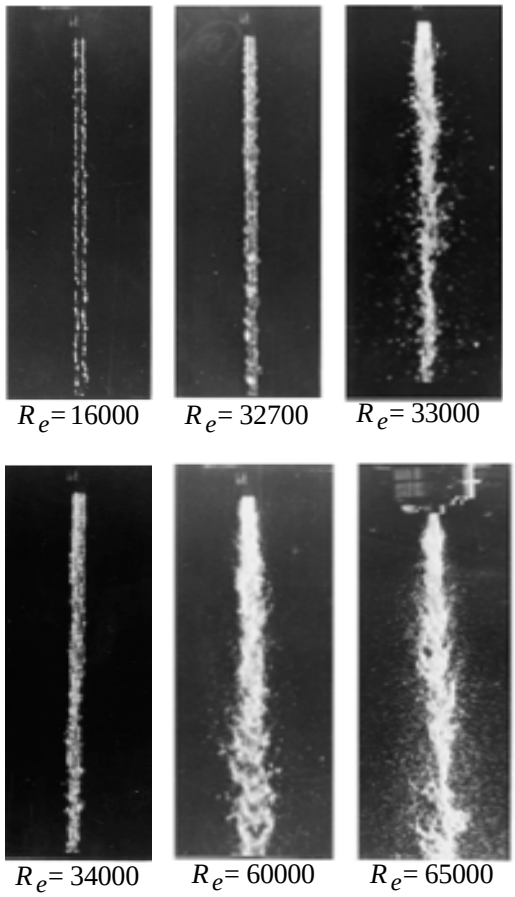

Figure 8. Jet structure at different Reynolds number for the 2-mm diameter orifice of aspect ratio 5 ($R_e = 33000$ corresponds to cavitation).

At the onset of cavitation, the structure of the jet abruptly changes especially for an aspect ratio of the orifice of 5. Figure 9 gives the photographs of liquid jets formed at the onset of cavitation for different aspect ratios for an orifice diameter of 2.5 mm. It is seen that the disintegration of the jet is most violent for an aspect ratio of 5. Globules of liquid are dispersed extensively suggesting that the disturbances induced in the jet by the orifice flow are maximum. The extent of such disturbances in the jet is lower at the onset of cavitation for orifices whose aspect ratios are less than or greater than 5 (Figure 9).

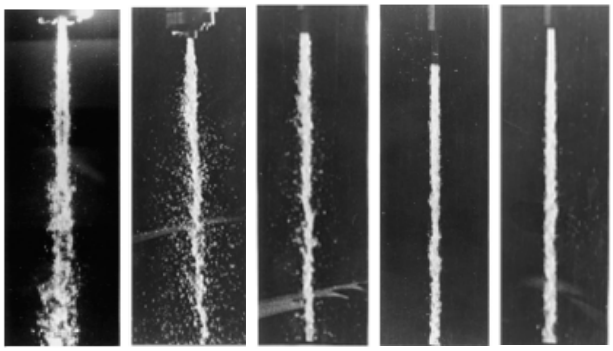

Figure 9. Jet structure at inception of cavitation for orifices with different aspect ratios (diameter of orifice = 2 mm).

The observation of the flow disturbances being higher for jets, formed from orifices with aspect ratio of about 5, has also been seen in the earlier experiments of Arai (Spikes and Pennington [9] and Ramamurthi and Nandakumar [24]). A study of the collapse of bubbles formed during cavitation for different orifice diameters is carried out in the following to infer the preference for the maximum cavitation disturbances to be obtained at the exit of the orifice when the aspect ratio is about 5. The generalised Rayleigh-Plesset equation for bubble dynamics given below is considered:

$$R\frac{d^2R}{dt^2} + \frac{3}{2}\left(\frac{dR}{dt}\right)^2 = \frac{1}{\rho}\left[(P_g - P_\infty) - \frac{2\sigma}{R} - \frac{4\mu}{R}\frac{dR}{dt}\right], \tag{11}$$

where P_g is the gas pressure in the bubble as it travels through the orifice and P_∞ is the pressure in the far field in the liquid. R is the radius of the bubble, σ is the surface tension and μ is the viscosity of the liquid.

The time for the bubble to collapse from the maximum radius of $R_{\max}$, at which dR/dt is 0, can be estimated neglecting the surface tension and viscosity terms in Equation (11) to give (Plesset and Prosperritti [31]):

$$t = 0.915R_{\max}\sqrt{\frac{\rho}{P_\infty - P_g}}. \tag{12}$$

The maximum radius of bubble can be assumed to correspond to the cavity volume due to formation of the vena contracta as shown in Figure 10. If d_v is the diameter of vena contracta, we have:

$$\frac{d_v^2}{d^2} \cong 0.62 \tag{13}$$

or

$$\frac{d_v}{d} \cong 0.8. \tag{14}$$

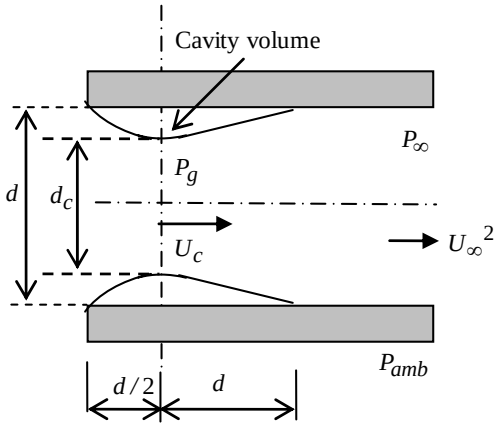

Figure 10. Schematic of flow separation.

Assuming incompressible fluid, the Bernoulli's equation for the velocities indicated in Figure 10 can be written as:

$$\frac{P_\infty}{\rho} + \frac{U_\infty^2}{2} = \frac{P_g}{\rho} + \frac{U_c^2}{2}, \tag{15}$$

where U_∞ is the free stream flow velocity after attachment and U_c is the velocity at vena contracta. Simplifying Equation (15) we get:

$$\frac{P_\infty - P_g}{\rho} = \frac{U_\infty^2}{2}\left[\left(\frac{d}{d_c}\right)^4 - 1\right]. \tag{16}$$

The time for collapse of the bubble from Equation (12) can be written as:

$$t = 0.915 R_{\max} \frac{\sqrt{2}}{U_\infty} \frac{1}{[(d/d_c)^4 - 1]^{1/2}}. \tag{17}$$

The value of $R_{\max}$ can be estimated assuming the bubble occupies the separation volume. It is expressed in terms of the diameters d_c and d as:

$$\frac{4}{3}\pi R_{\max}^3 \cong \frac{1}{8}\pi(d^2 - d_c^2)\left(\frac{d}{2} + d\right). \tag{18}$$

Since $d_c \cong 0.8d$, $R_{\max} = 0.37d$. Denoting $U_\infty t = l$ as the characteristic length over which the bubble collapses we have:

$$\frac{l}{d} = 0.915\sqrt{2}\,\frac{0.37}{[(d/d_c)^4 - 1]^{1/2}} \tag{19}$$

which gives $l/d = 0.40$.

The small value 0.4 of l/d is due to the rapid collapse of the bubble. Since the length over which flow contracts to vena contracta is about $d/2$ and the reattachment takes place over a distance of about a diameter, as schematically indicated in Figure 10, the length over which the cavitation bubble would collapse is:

$$\frac{l}{d} = 1.9. \tag{20}$$

Viscosity would increase the value of l/d at which the bubble would collapse. If we assume that the bubble would collapse at l/d of about 5, it would explain the maximum disturbance of the jet since implosion of the bubble at the exit of the orifice induces maximum disturbance to the jet. When the aspect ratio of the orifice (l/d) is higher than this value, the disturbances from the implosion are dissipated in the reattached flow region.

For aspect ratios less than about 4, the disturbances from the implosion are not available to disrupt the liquid jet strongly. This phenomenon would explain the preferential disintegration of the jet with cavitated flow for an aspect ratio around 5.

3.5. Flow hysteresis

The velocity at which cavitated flow ceases and returns to attached flow when the flow rates through the orifice are reduced is different from the

velocity at which the inception of cavitation is obtained. The direction of either increasing or decreasing flow rates decides the value of the discharge coefficients at a given value of Reynolds number. Figure 11 is a plot of the measured discharge coefficients for the 2.5 mm orifice when the flow was increased in steps to obtain cavitated flow and decreased thereafter. Here the discharge coefficients for aspect ratios of 5 and 10 are plotted. The Reynolds number at which the inception of cavitation occurs is higher than the Reynolds number at which the cavitated flow reverses back to the attached flow. The extent of the hysteresis zone along the Reynolds number axis is seen to be higher for the aspect ratio of 5. This result was also obtained by Ramamurthi and Nandakumar [32].

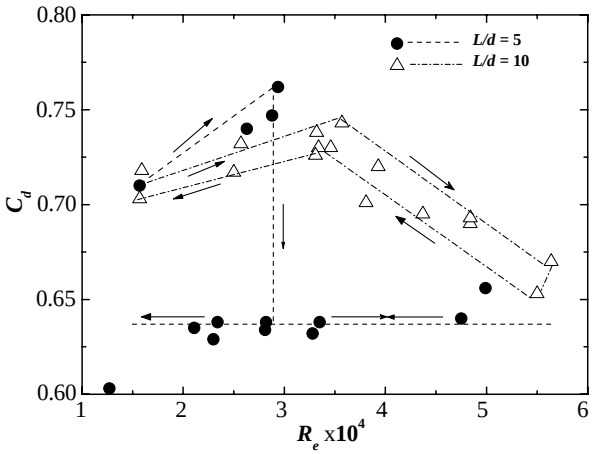

Figure 11. Hysteresis in C_d coefficient obtained for the 2mm diameter orifice of aspect ratios 5 and 10.

The hysteresis behaviour (Morrison and Edelman [33]) leads to different disintegration characteristics of the liquid jet from the same orifice at the same Reynolds number depending on whether the flow velocity is reached from the attached region of flow or the cavitated region of flow. The inertial force required to expel the cavitation bubble during the onset of cavitation is responsible for the higher Reynolds number at which the inception of cavitation takes place.

4. Conclusion

The discharge coefficients of sharp-edged cylindrical orifices scale with Reynolds number and aspect ratios in the case of attached noncavitating flows. For separated flows and flows with cavitation, the diameters of the orifice influence the discharge coefficients. Smaller diameter orifices give higher discharge coefficients in the separated flow region. The surface tension-induced pressures and increased wetting of the orifice walls lead to the increase of discharge coefficients. The values of discharge coefficients for separated and cavitated flows do not depend on Reynolds number.

The critical cavitation number is also dependent on the diameter of the orifice and the aspect ratio of the orifice. Orifices with an aspect ratio of about 5 give enhanced disturbances in the jet when the flow is cavitating. This seems likely due to the implosion of cavitation bubbles at the exit of the orifice. A model for collapse of bubbles qualitatively brings out this trend. Hysteresis is also observed in the flow. The detached flow after cavitation does not revert back to attached flow when the flow rate is reduced.

References

[1] J. M. Hobbs and J. S. Humphreys, The effect of orifice plate geometry upon discharge coefficient, Flow Measure. Instrument. 1(3) (1990), 133-140.

[2] T. R. Ohrn, D. W. Senser and A. H. Lefebvre, Geometrical effects on discharge coefficients for plain orifice atomizers, Atomiz. Sprays 1 (1991), 137-153.

[3] P. K. Wu, R. F. Miranda and G. M. Faeth, Effect of initial flow conditions on primary breakup of non turbulent and turbulent round liquid jets, Atomiz. Sprays 5 (1995), 175-196.

[4] L. C. Hollingshead, Discharge coefficient performance of venturi, standard concentric orifice plate, v-cone, and wedge flow meters at small Reynolds numbers, Master of Science in Civil and Environmental Engineering, Utah State University, Logan, Utah, 2011.

[5] A. Mansour and N. Chigier, Effect of turbulence on the stability of liquid jets and resulting droplet size distribution, Atomiz. Sprays 4 (1994), 583-604.

[6] N. Tamaki, M. Shimuzu, K. Nishida and H. Hiroyasu, Effects of cavitation and internal flow on atomization of a liquid jet, Atomiz. Sprays 8 (1998), 179-197.

[7] T. Kiljanski, Discharge coefficients for free jets from orifices at low Reynolds number, ASME J. Fluids Engineering 115 (1993), 778-781.

[8] I. D. Pearce and A. Lichtarowicz, Discharge performance of long orifices with cavitating flow, Proc. Second Fluid Power Symposium, January, Guildford Paper D2, University of Surrey, D2, 1971, pp. 13-35.

[9] R. H. Spikes and G. A. Pennington, Discharge coefficient of small submerged orifices, Proceedings of the Institution of Mechanical Engineers 173(1) (1959), 661-674.

[10] T. Hasegawa, M. Suganuma and H. Watanbe, Anomaly of excess pressure drops of the flow through very small orifices, Phys. Fluids 9 (1990), 1-3.

[11] N. Tamaki, M. Shimizu and H. Hiroyasu, Enhancement of the atomization of a liquid jet by cavitation in a nozzle hole, Atomiz. Sprays 11 (2000), 125.

[12] H. Hiroyasu, Spray breakup mechanism from the hole-type nozzle and its applications, Atomiz. Sprays 10 (2001), 511-527.

[13] K. Takahashi, H. Matsuda and H. Miyamoto, Cavitation characteristics of restriction orifices. CAV 2001: Fourth International Symposium on Cavitation, California Institute of Technology, Pasadena, 2001.

[14] Q. Y. Zhang and B. Q. Chai, Hydraulics characteristic of multiphase orifice tunnels, J. Hydraulic Engineering 127 (2003), 663-670.

[15] M. Chandan and P. Yoav, Cavitation in flow through a micro-orifice inside a silicon microchannel, Phys. Fluids 17 (2005), 013601.

[16] K. Ahn, J. Kim and Y. Yoon, Effects of orifice internal flow on transverse injection into subsonic crossflows: Cavitation and hydraulic flip, Atomiz. Sprays 16 (2006), 15.

[17] S. Dabiri, W. A. Sirignanoand and D. D. Joseph, Cavitation in an orifice flow, Phys. Fluids 19 (2007), 072112.

[18] M. Gavaises, D. Papoulias, A. Andriotis, E. Giannadakis and A. Theodorakakos, Link between cavitation development and erosion damage if diesel fuel injector nozzles, SAE Paper No. 2007-01-0246 (2007).

[19] E. Giannadakis, M. Gavaises and C. Arcoumanis, Modelling cavitation in diesel injector nozzle holes, J. Fluid Mech. 616 (2008), 153.

[20] E. Giannadakis, M. Gavaises and C. Arcoumanis, Modelling cavitation in diesel injector nozzle holes, J. Fluid Mech. 616 (2008), 153.

[21] E. Giannadakis, D. Papoulias, A. Theodorakakos and M. Gavaises, Simulation of cavitation in outward-opening piezo-type pintle injector nozzles, Proceedings of

the Institution of Mechanical Engineers, Part D: J. Automobile Engineering 222(10) (2008), 1895-1910.

[22] A. Andriotis and M. Gavaises, Influence of vortex flow and cavitation on near-nozzle diesel spray dispersion angle, Atomiz. Sprays 19 (2009), 247.

[23] T. Karasawa, M. Tanaka, K. Abe, S. Shiga and T. Kurabayashi, Effect of nozzle configuration on atomization of a steady spray, Atomiz. Sprays 2 (1992), 421-426.

[24] K. Ramamurthi and K. Nandakumar, Disintegration of liquid jets from sharp-edged orifices, Atomiz. Sprays 4 (1994), 551-564.

[25] S. Takahashi, Y. Yu and S. Yamaguchi, Study of unsteady orifice flow characteristics in hydraulic oil lines, ASME J. Fluids Engineering 118 (1996), 743-748.

[26] T. R. Ohrn, D. W. Senser and A. H. Lefebvre, Geometric effects on spray cone angle for plain-orifice atomizers, Atomiz. Sprays 1 (1992), 253-268.

[27] W. Bergwerk, Flow pattern in diesel spray holes, Proc. Inst. Mech. Eng. 173 (1993), 655-668.

[28] Y. Lang, Numerical study of inlet and geometry effects on discharge coefficients for liquid jet emanating from a plain-orifice atomizer, J. Mechanics 18 (2002), 153-161.

[29] Y. C. Wang and C. E. Brenn, One dimensional bubbly cavitating flows through a converging-diverging nozzle, ASME J. Fluids Engineering 20 (1998), 166-170.

[30] Z. Bikai, H. Yan, Z. Tiehua and L. Zhuangyun, Experimental investigation of the flow characteristics of small orifices and valves in water hydraulics, Proceedings of the Institution of Mechanical Engineers, Part E: J. Process Mechanical Engineering 216(4) (2002), 235-245.

[31] M. S. Plesset and A. Prosperritti, Bubble dynamics and cavitation, Ann. Rev. Fluid Mech. 9 (1977), 145-185.

[32] K. Ramamurthi and K. Nandakumar, Characteristics of flow through small sharp-edged cylindrical orifices, Flow Measure. Instrument. 10 (1999), 133-143.

[33] C. Morrison and A. Edelman, An experimental study of transient flow of liquids in LPG injectors, 24th JANNAF Combustion Meeting, Vol. 2, CPIA Publication 476 (1987), 67-77.